Electronic Supplementary Material (ESI) for Materials Advances.

Enhanced $LiMn_2O_4$ Cathode Performance in Lithium-Ion Batteries through Synergistic Cation and Anion Substitution

Oyunbayar Nyamaa[1], Hyo-Min Jeong[1], Gyeong-Ho Kang[3], Jung-Soo Kim[1], Kyeong-Mo Goo[1], In-Gyu Baek[1], Jeong-Hyeon Yang[2], Tae-Hyun Nam[3], Jung-Pil Noh[1] *

[1]Department of Energy and Mechanical Engineering and Institute of Marine Industry, Gyeongsang National University, 2 Tongyeonghaean-to, Tongyeong 53064, Korea

[2]Department of Mechanical System Engineering, Gyeongsang National University 2 Tongyeonghaean-to, Tongyeong 53064, Korea

[3]Department of Materials Engineering and Convergence Technology, Gyeongsang National University, Jinju-daero 501, Jinju 52828, Korea*

*Corresponding author Email: nohjp@gnu.ac.kr

Contents

1. Introduction

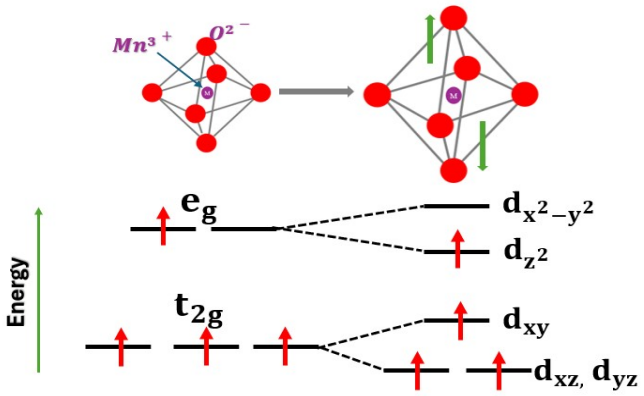

$Jahn-Tellor\ distortion\ for\ HS\ d^4\ Mn^{3+}$

Fig.S1 The Jahn-Teller distortion induces changes in the splitting pattern and occupation of the d-orbital set of Mn^{3+}. Initially in an octahedral coordination environment, and subsequently in a tetragonally elongated complex resulting from the Jahn-Teller effect, alterations occur in the arrangement and occupancy of the Mn^{3+} d orbitals.

2. Experimental details

Using previous research findings, it demonstrated a decrease in capacity when replacing Ti with active Mn ions at levels exceedingly approximately 0.5, and there is still a loss of capacity in cycle life at excessively low levels [1-3]. Given the limited research on contents of Ti, we have examined the synergistic cation and anion substitution at contents of Ti that were previously unexplored. Therefore, to precisely optimize the substitution ions in the study, particles with 2 types of Ti ion content were prepared. The preparation of the particles follows the identical sol-gel method employed in the $LiMn_2O_4$, Ti substituted $LiMn_2O_4$, and Ti-S substituted $LiMn_2O_4$ nanoparticles section (Fig. 1). The molar ratios of oxygen (O), manganese (Mn), and titanium (Ti) are determined

through EDS analysis, utilizing their respective atomic percentages (at. %). This analysis yields the molar ratio calculation for $LiMn_{1.85}Ti_{0.15}O_4$ (Ti-0.15) and $LiMn_{1.78}Ti_{0.22}O_4$ (Ti-0.22). The prepared cathodes contained the zero amount of S, differing only in the content of Ti ions, and were named T-0.15 and Ti-0.22 based on content of Ti. Fig. S2 shows the cycling performance of cathodes at 1C for 100 cycles. The initial discharge capacity of both cathodes was 121 and 134 mAh/g for Ti-0.15 and Ti-0.22, along with corresponding Coulombic efficiencies are 96.3% and 96.9%, respectively. The capacity retention of cathodes was 84.4% and 83.5% for Ti-0.15 and Ti-0.22. As a result, the content of Ti-0.22 was a more suitable value (higher initial capacity and similar capacity retention) for stabilizing the structure and was chosen further in the study.

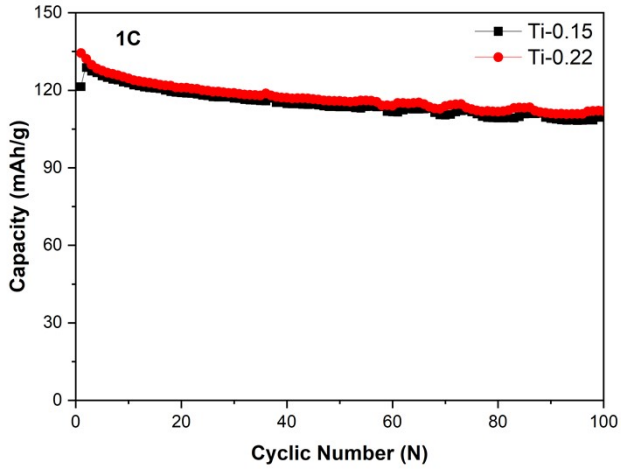

Fig. S2. Charge/discharge capacity profiles of (black curve) $LiMn_{2-x}Ti_xO_4$ $x < 0.15$, and (red curve) $LiMn_{2-x}Ti_xO_4$ $x < 0.22$ upon 100 cycles over a cut-off voltage range of 4.3-3.1 V at 0.5 C.

3. Characteristics of the particle

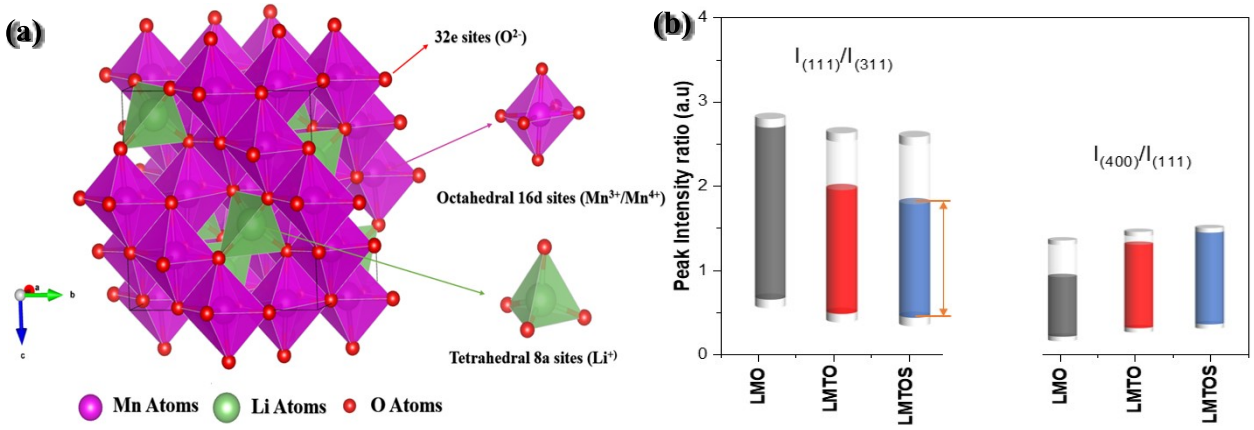

Fig. S3 Illustrated in (a) is a schematic representation of the crystalline structure of spinel $LiMn_2O_4$, showcasing the unit cell with atomic bonds and metal sites. Within this representation, Mn1 positioned at 16d is denoted by a pink atom, Li1 at 8a is represented by a green atom, and oxygen is indicated by small (red) atoms, providing insight into the cubic spinel $LiMn_2O_4$ crystal structure. The ratios of (b) peak intensities, specifically $I_{(111)}/I_{(311)}$and $I_{(400)}/I_{(111)}$ from the

XRD patterns depicting crystal facets, were extracted for the synthesized particles. The comparison cylinder uses the highest ratio, LMO particle, as the basis for calculating the $I_{(111)}/I_{(311)}$ ratios, while for $I_{(400)}/I_{(111)}$, the highest peak intensity ratio of LMTOS particle used to compare peak intensity ratio of particles.

4. Electrochemical result

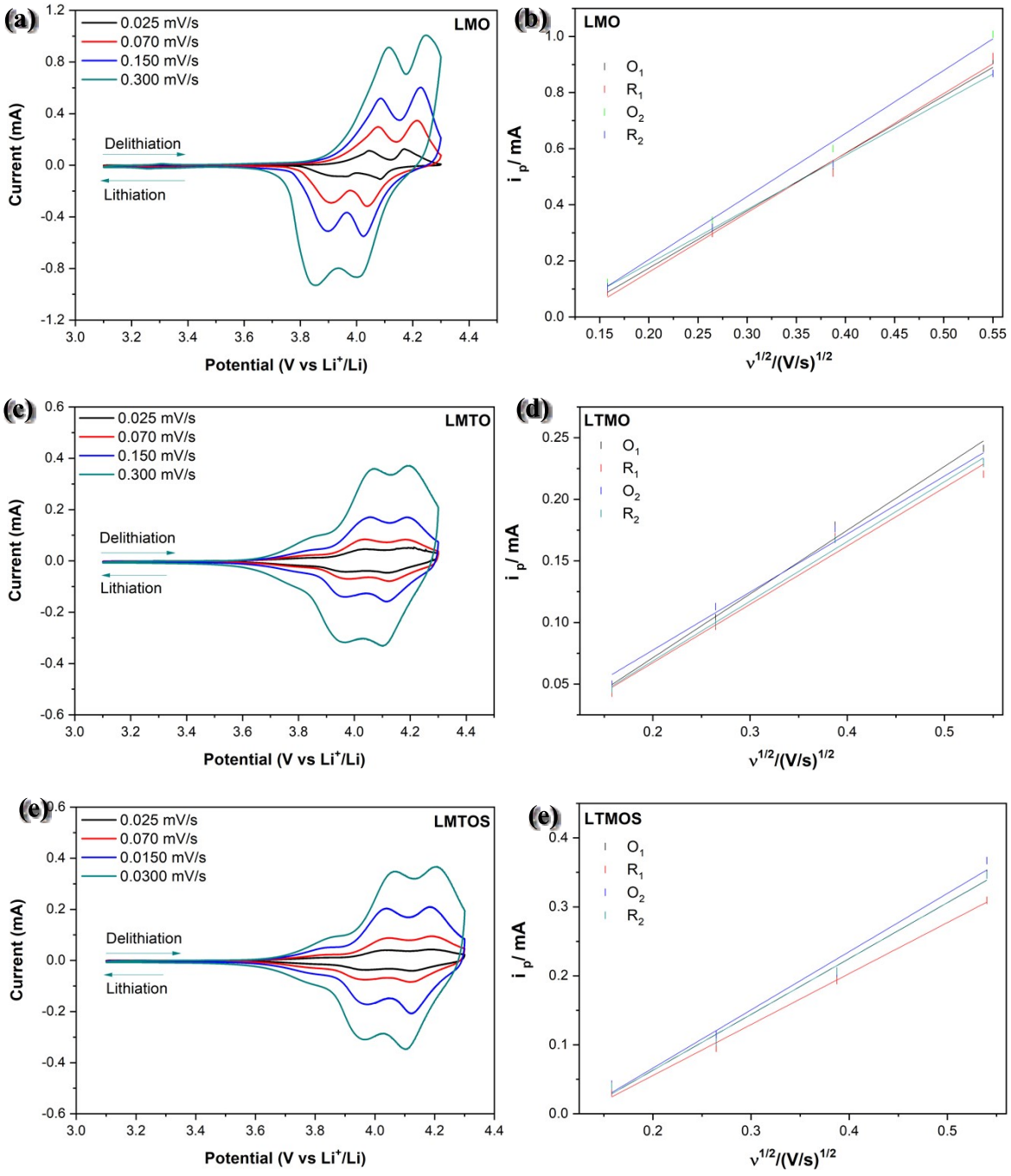

Fig. S4 Cyclic voltammetry (CV) curves for LMO (a), LMTO (c), and LMTOS (e) at different scan rates in the voltage range of 3.1- 4.3 V. The scan rates vary from 0.025 to 0.30 mV s^{-1}.

The oxidation peaks are noted O_1 and O_2 while the reduction peaks are noted R_1 and R_2. The linear relationship of peak current (I_p) vs square root of the scan rate ($v^{1/2}$) for LMO (b), LMTO (d), and LMTOS (f). The linear fitting is according to Eq. 2

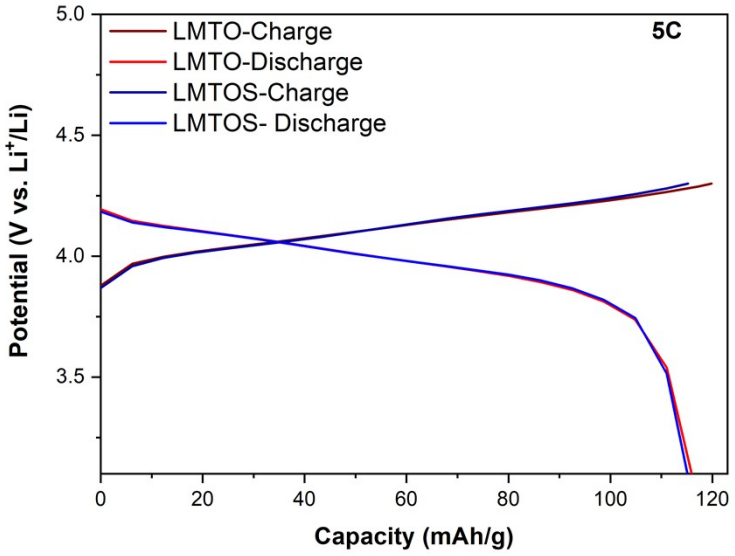

Fig. S5 Charge/discharge capacity profiles of cathodes in 1st cycle at cut-off voltages of 4.3−3.1 V (5C).

Table. S1 Lithium Diffusion Coefficients (D_{Li}) calculated from the CV test for the three cathodes.

Samples	**O_1**	**O_2**	**R_1**	**R_2**	**Average D_{Li} ($cm^2\ s^{-1}$)**
LMO	1.95×10^{-9}	2.17×10^{-9}	1.95×10^{-9}	1.93×10^{-9}	8.1×10^{-10}
LMTO	7.30×10^{-10}	7.41×10^{-10}	6.34×10^{-10}	6.72×10^{-10}	6.4×10^{-10}
LMTOS	8.12×10^{-10}	8.5×10^{-10}	5.45×10^{-10}	8.11×10^{-10}	7.9×10^{-10}

References

(1) Callegari, D.; Coduri, M.; Fracchia, M.; Ghigna, P.; Braglia, L.; Tamburini, U. A.; Quartarone, E. Lithium intercalation mechanisms and critical role of multi-doping in LiFe x Mn 2− x− y Ti y O 4 as high-capacity cathode material for lithium-ion batteries. *Journal of Materials Chemistry C* **2022**, *10* (23), 8994-9008.

(2) Wang, S.; Yang, J.; Wu, X.; Li, Y.; Gong, Z.; Wen, W.; Lin, M.; Yang, J.; Yang, Y. Toward high capacity and stable manganese-spinel electrode materials: A case study of Ti-substituted system. *Journal of Power Sources* **2014**, *245*, 570-578.

(3) Zhang, Y.; Xie, H.; Jin, H.; Li, X.; Zhang, Q.; Li, Y.; Li, K.; Luo, F.; Li, W.; Li, C. Enhancing the electrochemical properties of Ti-doped LiMn2O4 spinel cathode materials using a one-step hydrothermal method. *ACS omega* **2021**, *6* (33), 21304-21315.